Photoinduced Processes in Highly Coupled Multicomponent Arrays Based on a Ruthenium(II)Bis(terpyridine) Complex and Porphyrins

Lucia Flamigni,* Francesco Barigelletti, Nicola Armaroli, Jean-Paul Collin,* Jean-Pierre Sauvage,* and J. A. Gareth Williams

Abstract: A new multicomponent array (**PH_2-Ru-PAu**) has been synthesized, consisting of a free-base arylporphyrin and a gold(III) arylporphyrin, assembled together with a central ruthenium(II)-bis(terpyridine) complex. The photophysical properties of this triad, of the molecular models and of the related dyads **Ru – PH_2** and **Ru – PAu** have been determined by steady-state and time-resolved methods. Excitation of the **Ru – PH_2** array in the porphyrin subunit results in energy transfer from the porphyrin singlet to the ^{3}MLCT-excited level of the ruthenium complex ($k = 2.4 \times 10^9\,s^{-1}$), followed by a very fast ($k > 5 \times 10^{10}\,s^{-1}$) energy transfer to the porphyrin-localized triplet state with an efficiency close to unity. The role of the ruthenium in perturbing the spin multiplicity of the excited states is essential to promote the fast energy transfer between the free-base porphyrin singlet and the lowest MLCT excited state of the complex, which is formally a triplet. Excitation of the **Ru – PAu** dyad in the MLCT manifold of the ruthenium complex yields the porphyrin-localized triplet within our experimental resolution (20 ps) with unit efficiency. No evidence of photoinduced electron transfer emerges from our data and the observed processes are essentially ascribed to energy transfer by a Dexter-type mechanism. In the **PH_2-Ru-PAu** triad excitation in the free-base-porphyrin subunit produces the excited singlet state, which is quenched with a rate $k = 5.6 \times 10^9\,s^{-1}$. The quenching is assigned to energy transfer by a Dexter mechanism to the ^{3}MLCT state of the ruthenium complex, which in turn transfers triplet energy very rapidly ($k > 5 \times 10^{10}\,s^{-1}$) to the gold porphyrin and to the free-base porphyrin units with an efficiency ratio of four. The overall quantum yield of porphyrin triplets is unity. Direct excitation in the MLCT manifold of the complex causes a similar photoinduced energy transfer to the peripheral porphyrins. Excitation of the gold(III) porphyrin in the triad produces the corresponding triplet, which is unable to promote the thermodynamically allowed triplet energy transfer to the spatially opposite free-base porphyrin. The prevalence of energy-transfer processes with respect to thermodynamically allowed electron transfer in this and related systems is discussed on the basis of the nature of the metal complex and of current theories.

Keywords: electrochemistry · photoinduced processes · porphyrins · ruthenium · supramolecular chemistry

Introduction

Porphyrin type components have been widely used in multicomponent arrays to promote photoinduced energy- or electron-transfer processes.[1] The most important reasons for such investigations arise from the interest in mimicking natural photosystems,[1a–d] the successful strategies proposed to attach the tetrapyrrolic ring both by covalent[1–6] or noncovalent[7–14] bonds to suitable molecular entities and the high extinction coefficients throughout the visible region. In addition, the intermediates involved in the photoinduced processes are relatively easy to detect by optical spectroscopic techniques.[4–12, 15–19, 22]

Our synthetic work has been aimed at the construction of molecular assemblies with rigid geometries based on porphyrins and transition metal complexes.[1d] In particular a new strategy has been designed based on the templating effect of a transition metal cation (generally Ru^{II}) to assemble two porphyrinic components in a rigid and linear array.[19b–c, 20] The resulting triad, properly functionalized, should be suitable for use as a building block for more complex linear entities to achieve photoinduced vectorial electron or energy transport over long distances.

Previous work on molecular triads, consisting of a ruthenium(II)bis(terpyridyl) unit covalently linked to either a zinc(II) or free-base porphyrin as the terminal group on one side and a gold(III) porphyrin on the opposite side, indicates

---

[*] Dr. L. Flamigni, Dr. F. Barigelletti, Dr. N. Armaroli
Istituto di Fotochimica e Radiazioni d'Alta Energia del C. N. R.
via P Gobetti 101, I-40129 Bologna (Italy)
Fax: (+39) 51-639-9844
E-mail: flamigni@bofra3.frae.bo.cnr.it
Dr. J.-P. Collin, Dr. J-P. Sauvage, Dr. J. A. G. Williams
Laboratoire de Chimie Organo-Minérale, URA CNRS 422
Université Louis Pasteur, Faculté de Chimie
4 rue Blaise Pascal, 67070 Strasbourg (France)

0947-6539/98/0409-1744 $ 17.50+.50/0

the formation of a charge-separated state over the centre-to-centre 30 Å distance separating the terminal porphyrins.[19c] In that case, the photoinduced electron transfer occurred from the excited state of the zinc or free-base porphyrin to the metal complex, followed by a secondary thermal electron transfer to the appended gold(III) porphyrin. Direct photoinduced electron transfer between opposite porphyrins did not occur in spite of the favourable driving force, neither from the free-base or zinc(II) porphyrin singlet, nor from the excited gold(III) porphyrin triplet. The poor ability of the central Ru complex in promoting electronic coupling between the extreme components was identified as the reason for the inefficiency of such direct electron transfer between terminal units during the porphyrin excited state lifetime. The same reason was put forward for the inefficiency of triplet energy transfer between the extreme porphyrins.

Abstract in Italian: *E'stata sintetizzata una nuova struttura sopramolecolare costituita da due aril porfirine, di cui una a base libera e l'altra metallata con oro(III), assemblate mediante un complesso centrale bis-terpiridinico di rutenio(II),* ***PH$_2$-Ru-PAu****. Le proprietà fotofisiche della triade, dei modelli molecolari e delle relative diadi* ***Ru-PH$_2$*** *e* ***Ru–PAu****, sono state determinate mediante metodi stazionari e risolti nel tempo. L'eccitazione del sistema* ***Ru–PH$_2$*** *nella sottounità porfirinica ha come risultato un trasferimento di energia dallo stato di singoletto della porfirina allo stato eccitato ^{3}MLCT del complesso di rutenio ($k = 2.4 \times 10^9$ s^{-1}) seguito da un velocissimo ($k > 5 \times 10^{10}$ s^{-1}) trasferimento di energia al tripletto localizzato sulla porfirina con un efficienza quasi unitaria. Il ruolo del rutenio nel perturbare la molteplicità di spin dello stato eccitato è essenziale per promuovere il rapido trasferimento di energia fra lo stato di singoletto della porfirina a base libera ed il più basso stato eccitato MLCT del complesso, che è formalmente un tripletto. L'eccitazione della diade* ***Ru–PAu*** *nella banda MLCT del complesso di rutenio produce lo stato di tripletto localizzato sulla porfirina in tempi minori della nostra risoluzione strumentale (20 ps) con efficienza unitaria. Dai dati disponibili non si ha evidenza di processi di trasferimento elettronico ed i processi osservati sono essenzialmente attribuiti a trasferimento di energia che ha luogo con un meccanismo di tipo Dexter. Nella triade* ***PH$_2$-Ru-PAu****, l'eccitazione nella subunità porfirina a base libera dà luogo allo stato eccitato di singoletto che viene spento con una costante di velocità $k = 5.6 \times 10^9$ s^{-1}. Lo spegnimento è attribuito a trasferimento di energia, con un meccanismo di tipo Dexter, allo stato ^{3}MLCT del complesso di rutenio che a sua volta trasferisce energia di tripletto molto rapidamente ($k > 5 \times 10^{10}$ s^{-1}) alla oro(III) porfirina ed alla porfirina a base libera con un rapporto nelle rispettive efficienze pari a 4. La resa complessiva di tripletto delle porfirine è unitaria. Eccitazione diretta nella banda MLCT del complesso ha come risultato un analogo trasferimento di energia alle porfirine periferiche. Eccitazione della oro(III) porfirina nella triade risulta nella formazione del corrispondente tripletto che non è in grado di trasferire energia alla porfirina a base libera che si trova alla estremità opposta, nonostante sia termodinamicamente favorevole. La prevalenza, in sistemi di questo tipo, di processi di trasferimento di energia rispetto a trasferimento di elettrone termodinamicamente consentiti, è discussa sulla base della natura del complesso metallico e delle teorie correnti.*

A subsequent approach was aimed at substituting the chemically fragile etioporphyrin used in the previous study with the more robust tetraphenyl free-base or zinc derivatives.[21, 22] As the latter is less electron rich, a Ru^{II}-terpyridyl derivative more prone to reduction was used in order to maintain the driving force for charge separation. The Ru^{II} complex used in this case turned out to perform as a drain for the energy delivered to the system and, because of the extremely short intrinsic lifetime of its excited state, was unable to perform any useful act. The outcome of this study was quite different from the one discussed above.[19b–c] Our main result was the preponderance of energy-transfer processes between formally spin-forbidden states that was made feasible as a result of the perturbing heavy-atom effect. This result, compared with the previous ones,[19] shows the large influence on the overall performance of a complex structure brought about by very small changes in the engineering of the molecular structure.

Our present interest is to substitute the etioporphyrin of the previously synthesized molecular triads with a more robust arylporphyrin and to try to increase the electronic coupling between peripheral porphyrins in order to promote direct electron and energy transfer. This is achieved by the preparation of a linear triad consisting of free-base and gold(III) triarylporphyrins as terminal groups, with the fourth meso position of each porphyrin attached directly to the terpyridyls coordinating the central Ru^{II} (Figure 1). Substitution of etio- with arylporphyrins should improve the robustness of the system as compared with the previously synthesized Ru^{II} triad[19c] and, owing to the less electron-rich nature of the arylporphyrin, prevent the electron-transfer step from the porphyrin singlet to the metal complex, by increasing the endoergonicity of this process. The direct connection of the π-porphyrin system to the ligand orbitals should improve the electronic communication between the terminal porphyrins, thereby promoting the direct electron and/or energy transfer between them. In fact, energy transfer between triplets occurs by the Dexter mechanism,[23] which can itself be regarded as a double-electron exchange affected by similar parameters to those determining electron transfer.

The present work reports on the synthesis, spectroscopy, electrochemistry and photophysical properties of the new molecular triad **PH$_2$-Ru-PAu,** the reference dyads **Ru–PH$_2$** and **Ru–PAu**, the model compounds for the ruthenium complex **Ru** and **Ru'** and the porphyrins **PH$_2$** and **PAu**. The schematic formulae of the investigated compounds are shown in Figure 1.

Results and Discussion

The models: The choice of a proper model for the Ru complex moiety is not straightforward. The photophysical properties of bis(terpyridine)ruthenium complexes are in fact known to be highly dependent on the nature of the substituents, partic-

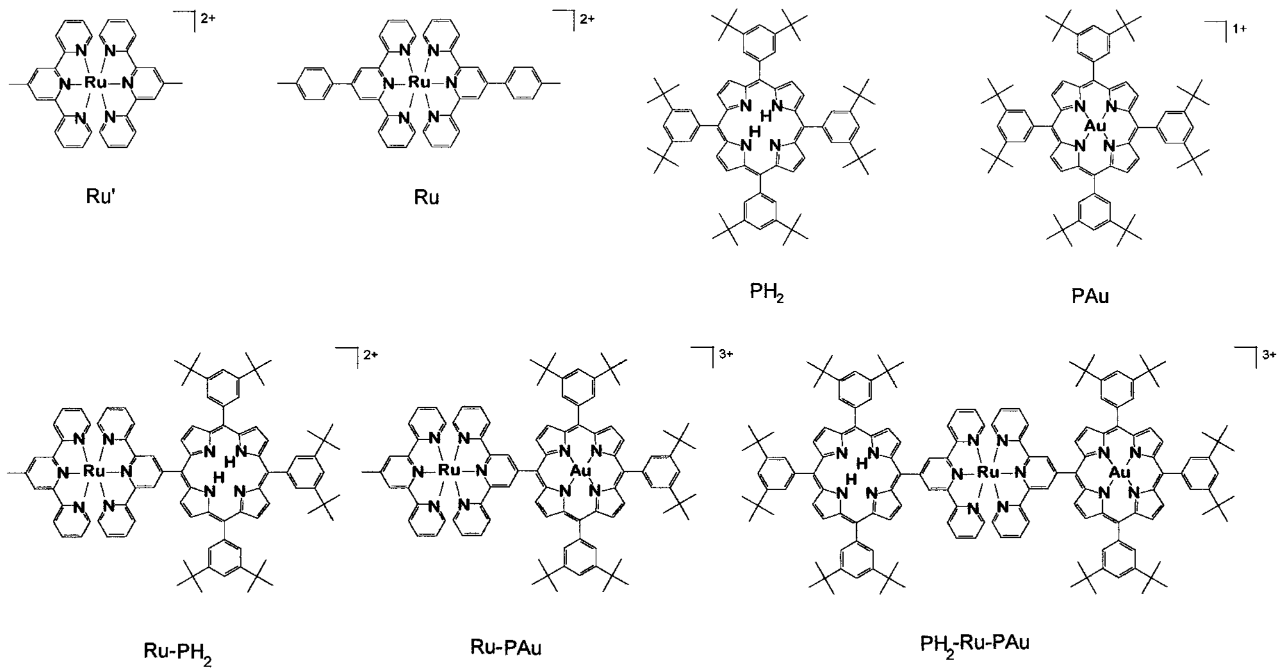

Figure 1. Schematic formulae of compounds studied.

ularly at the 4′ position of the ligand.[24, 25] In particular, the excited-state lifetime of the complex at room temperature can vary by several orders of magnitude and the energy level of the lowest excited state can vary by fractions of eV. Among other factors, the electron-withdrawing and -releasing properties of the substituents, or the presence of available protonation sites or groups that can promote the electronic delocalization of the ligand can affect the ^{3}MLCT excited-state properties.[25, 26]

The right model for our case should possess a substituent which can mimic the electronic environment of the meso position of the porphyrins. We used $[Ru(ttpy)_2]^{2+}$ (**Ru;** ttpy = 4′-(*p*-tolyl)-2,2′:6′,2″-terpyridine) as a model, because of the aromatic environment offered to the 4′ position by the tolyl substituent, similar to the meso position of porphyrins. In the dyads, in which a methyl group is the substituent opposite to the porphyrin, the $[Ru(ttpy)_2]^{2+}$ model could be less appropriate, therefore we also examined $[Ru(4'\text{-methylterpyridine})_2]^{2+}$ (**Ru′**) in order to be able to evaluate critically the pertinence of the model to the relevant supramolecular structure.

Synthesis of the ligands and complexes: 4′-methylterpyridine was prepared as described previously[19b] and oxidized to 4′-formylterpyridine with selenium oxide. The terpyridine-appended porphyrin (previously prepared by the Adler method[19b]) was prepared following the general procedure of Lindsey[27] in 11 % yield. The symmetrical porphyrin **PH$_2$** was obtained in substantial quantities as a by-product of this reaction. Metallation of the porphyrins with gold was carried out under acidic conditions (glacial acetic acid) to inhibit competitive complexation to the terpyridine group. The formation of the ruthenium complexes, the dyads and triad makes use of the mild dechlorination procedure established recently.[19b] In the first step, the terpyridine or porphyrin-appended terpyridine (L) is treated with ruthenium trichloride to give $RuLCl_3$. This is subsequently dechlorinated by reaction with silver tetrafluoroborate or silver triflate in acetone solution to yield the solvated complex $[RuL(acetone)_3]^{3+}$. Reaction with the appropriate second terpyridine in refluxing ethanol under inert atmosphere leads to the asymmetrical bis(terpyridine)ruthenium complex. In each case, anion exchange to form the PF_6^- salt was carried out prior to purification by column chromatography on silica with highly polar eluants.

Electrochemical behaviour: The redox potentials obtained in BuCN are compiled in Table 1 for the dyads **Ru–PAu**, **Ru–PH$_2$**, the triad **PH$_2$-Ru-PAu** and reference compounds **Ru**, **Ru′**, **PH$_2$** and **PAu**. Reversible monoelectronic waves were observed in almost all redox processes. In the dyads and the triad, the different reversible waves can be easily assigned to their individual components, Ru and PH$_2$ (or PAu) indicating ruthenium-complex and porphyrin-centred redox processes, respectively. Concerning the reference compounds **Ru**, **PH$_2$**, and **PAu**, the cyclic voltammogram curves display the usual oxidation and reduction processes as previously reported.[24, 19c, 22] A small effect due to the methyl group (electron donor) in 4′ position of the terpyridine in **Ru′** leads to a slightly less positive oxidation potential and a more negative reduction potential as compared with the redox potentials of **Ru**. In the triad and the dyads, some interaction is expected between the ruthenium complex and the porphyrinic components due to the close proximity of the different subunits. Since the porphyrinic units are electron-withdrawing groups, the oxidation potential of the ruthenium complex moves to more positive potential. This effect seems to be negligible on the reduction potential of the terpyridine ligands. The influence of the ruthenium complex (as an acceptor group) on the redox behaviour of the porphyrinic subunits is

0947-6539/98/0409-1746 $ 17.50+.50/0

Table 1. Redox Potentials in butyronitrile.

	Oxidation $E_{1/2}$ [V vs SCE]			Reduction $E_{1/2}$ [V vs SCE]					
Ru	1.33						-1.11	-1.36	
Ru′	1.31						-1.18	-1.42	
PH_2		1.33[a]	1.11			-1.07			-1.48
PAu				-0.47	-1.02				
Ru–PH_2	1.41	1.27	1.07			-0.96	-1.07	-1.39	-1.65
	Ru	PH_2	PH_2			PH_2	Ru	Ru	PH_2
Ru–PAu	1.37			-0.41	-0.87		-1.18	-1.42	
	Ru			PAu	PAu		Ru	Ru	
PH_2-Ru-PAu	1.44	1.20[b]		-0.42	-0.86	-0.97	-1.17	-1.40	-1.67
	Ru	PH_2		PAu	PAu	PH_2	Ru	Ru	PH_2

[a] Poorly defined wave. [b] Two overlapped waves.

particularly discernible on the reduction waves. The addition of the first electron to the porphyrin ring is easier in the case of the dyads and the triad as compared with the porphyrin models. The modification of the redox potentials in the dyads and the triad (in the order of 100 mV or less) expresses a relatively low interaction between each component resulting from a mutual electronic effect. As a consequence, the usual approach based on a localized description of the individual components seems reasonable in first approximation.

Steady state spectroscopic determinations: The absorption maxima with the calculated molar absorption coefficients for the models and the arrays are reported in Table 2. The absorption spectrum of **Ru–PAu** superimposed with the sum of the spectra (molar absorption coefficients) of the model components is shown in Figure 2. **Ru** and **Ru′** are alternatively used as models for the complex. The absorption spectrum of the triad **PH_2-Ru-PAu**, superimposed with the individual components **Ru, PH_2** and **PAu** and their sum, is given in Figure 3.

Table 2. Absorption maxima in butyronitrile.

	λ_{max} [nm] ($\varepsilon \times 10^{-4}$ [$M^{-1}cm^{-1}$])					
Ru	490 (3.35)					
Ru′	479 (1.61)					
PH_2		419 (49.5)	516 (1.70)	551 (0.99)	592 (0.49)	648 (0.53)
PAu		413 (36.5)	524 (1.77)	560 (0.29)[a]		
Ru–PH_2	485 (3.58)	421 (23.48)	517 (2.86)	557 (1.64)	592 (0.76)	649 (0.65)
Ru–PAu	485 (2.89)	412 (22.02)	525 (2.43)			
PH_2-Ru-PAu	490 (4.75)	416 (30.60)	522 (4.42)	557 (2.17)	585 (0.98)	649 (0.60)

[a] Shoulder.

From these data it is evident that the metal complex in the dyads is better described by an average of **Ru** and **Ru′** properties, while the complex in the triad is better described by **Ru**. As far as the MLCT transitions of the complex and the Q bands of the porphyrins are concerned, both the position and the intensity of the bands in the arrays appear to be affected only to a very modest extent with respect to the models, while a larger effect can be detected on the Soret bands of the porphyrins and the ligand centred bands of the complex (see Figure 3 and Table 2).

We were unable to detect any emission from **Ru′** solutions at room temperature by steady state techniques. At 77 K the emission is intense and centred at 604 nm. **Ru** displays a weak luminescence at room temperature ($\lambda_{max} = 640$ nm) that is strongly enhanced at 77 K ($\lambda_{max} = 628$ nm), in agreement with previous reports.[24] **PAu** does not fluoresce; only a phosphorescence peak at 710 nm can be detected in glassy solutions at 77 K. **PH_2** fluoresces strongly ($\Phi = 0.19$[19a]) at room temperature and in glassy solutions at 77 K (Table 3).

At room temperature, upon excitation of the **Ru–PH_2** dyad and the **PH_2-Ru-PAu** triad, the only detectable luminescence is due to the free-base porphyrin, which is quenched with respect to the model (Figure 4). The excitation spectrum, measured with an emission wavelength equal to that of the porphyrin fluorescence, overlaps the absorption spectrum of the free-base porphyrin.

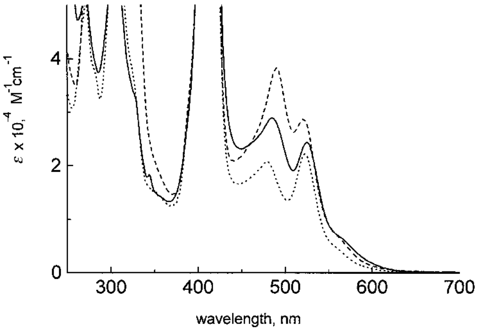

Figure 2. Absorption spectra of butyronitrile solutions of the **Ru–PAu** dyad (—), **Ru** + **PAu** (- - -) and **Ru′** + **PAu** (⋯⋯).

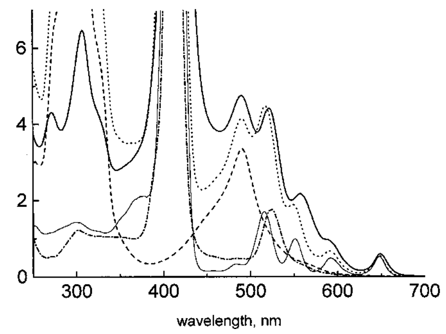

Figure 3. Absorption spectra of butyronitrile solutions of the **PH_2-Ru-PAu** triad (—), **PH_2** + **Ru** + **PAu** (⋯⋯), **Ru** (- - -), **PH_2** (—) and **PAu** (-·-·-·).

Table 3. Emission properties in butyronitrile.

	298 K			77 K	E [eV][d]
	λ_{max} [nm]	τ [ns]	Φfluo	λ_{max} [nm]	
Ru	640	0.7[a]	–	628	1.97
Ru′	620[a]	0.04[a]	–	604	2.05
PH_2	651	8.3	0.19[b]	647	1.92
PAu				710	1.75
Ru–PH_2	654	0.4[a]	0.006	643	1.93
Ru–PAu				700	1.77
PH_2-Ru-PAu	653	0.175[a]	0.003	645	1.92
				710[c]	1.75

[a] Streak camera. [b] From ref. [19a]. [c] Very weak signal. [d] Energy level from the emission maxima at 77 K.

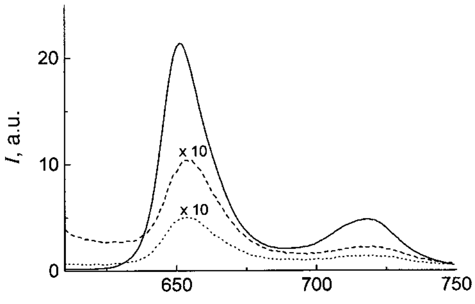

Figure 4. Emission spectra of butyronitrile solutions of **PH_2** (—), **Ru–PH_2**(- - -) and **PH_2-Ru-PAu** (·····). The excitation wavelengh is 598 nm, at which the solutions have equal absorbances.

The phosphorescence signal of the gold porphyrin can be detected in **Ru–PAu** dyad at 77 K, but it is practically absent in the triad **PH_2-Ru-PAu** (Figure 5). The excitation spectrum, measured with an emission wavelength equal to that of the PAu phosphorescence in **Ru–PAu**, overlaps the absorption spectrum of the dyad, showing also the typical MLCT band of the Ru-complex. Emission data are given in Table 3.

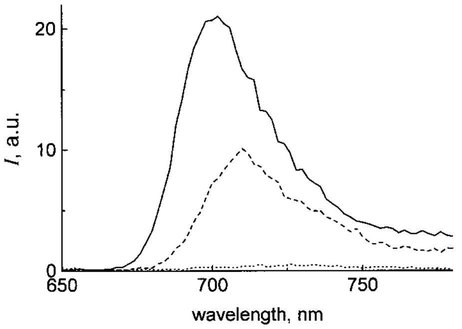

Figure 5. Phosphorescence spectra at 77 K of butyronitrile solutions of **PAu** (- - -), **Ru–PAu** (—), and **PH_2-Ru-PAu** (·····). The excitation wavelengh is 420 nm.

Time-resolved luminescence: The lifetimes of the PH_2 fluorescence in the model, in the dyad and in the triad were measured to be 8.3 ns, 400 ps and 175 ps, respectively, at room temperature, in reasonable agreement with the reduction in the luminescence yields measured by steady state spectroscopy. The emission of the **Ru′** model at room temperature, which could not be detected by the steady state method, was registered with a streak camera and displays a maximum at 620 nm with a lifetime of 40 ps (Figure 6). The model **Ru** displays an emission with maximum at 640 nm and a lifetime of 700 ps at room temperature.

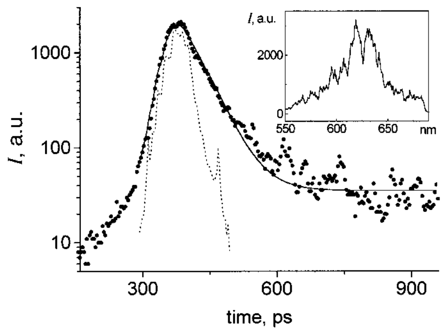

Figure 6. Emission decay profile for **Ru′** solutions in butyronitrile. The exponential fit corresponding to $\tau = 40$ ps (—), and the excitation profile (·····) are also shown. In the inset, the emission spectral profile detected in the time interval 0–50 ps is reported.

The attempt to determine the luminescence lifetime of the ruthenium complex at room temperature from **Ru–PAu**, **Ru–PH_2** and the triad was unsuccessful since no signal attributable to **Ru** or **Ru′** could be registered by the streak camera. While this may be expected in the PH_2-containing dyad and the triad, in which the luminescence from the free base can overshadow the weaker emission from the complex, the absence of such emission in the **Ru–PAu** dyad in a totally dark spectral region is indicative of the fact that the quenching is faster than our detection limit ($\tau < 20$ ps, $k > 5 \times 10^{10}$ s^{-1}). The data related to luminescence lifetimes are given in Table 3.

Time-resolved absorbance: Both ruthenium complexes show a transient absorbance with a negative signal corresponding to the bleaching of the ground state ^{1}MLCT absorption band and two positive absorbances around 400 nm and 600 nm. As can be seen by the spectra of Figure 7, obtained under similar experimental conditions, the intensity of the absorption signal is reduced for **Ru′** with respect to **Ru** by one order of magnitude. The lifetimes are 40 ps and 680 ps for **Ru′** and **Ru**,

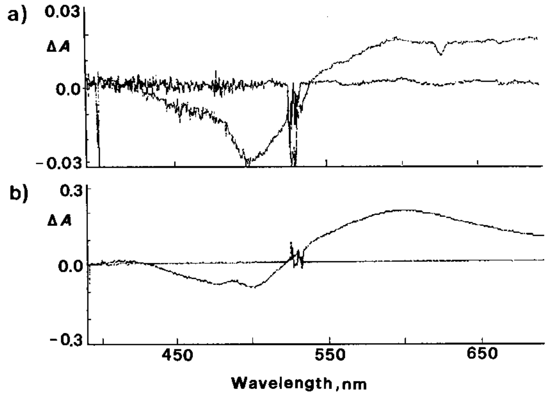

Figure 7. Differential transient absorption spectra at the end of a 35 ps pulse of butyronitrile solutions of **Ru′** (a) and **Ru** (b). The experimental conditions are the same.

respectively, and are in excellent agreement with the lifetimes derived by luminescence decay.

Picosecond flash photolysis of **PH_2** shows the typical singlet absorption band ($\lambda_{max} = 440$ nm) that only very partially evolves to triplet on the time scale of this experiment (0–3 ns). The fully evolved triplet absorbance can be detected with a nanosecond-flash-photolysis apparatus and displays an intense band at 450 nm with a weaker tail extending over 800 nm, characterized by the bleaching signals of the ground state Q bands. In deaerated solutions the lifetime of the **PH_2** triplet is 200 µs.

The triplet absorbance can be detected after excitation of BuCN solutions of **PAu**; it is characterized by bands at 445 nm, 610 nm and 770 nm, and a lifetime of 1.4 ns. The 550–850 nm wavelength region is displayed in Figure 8a.

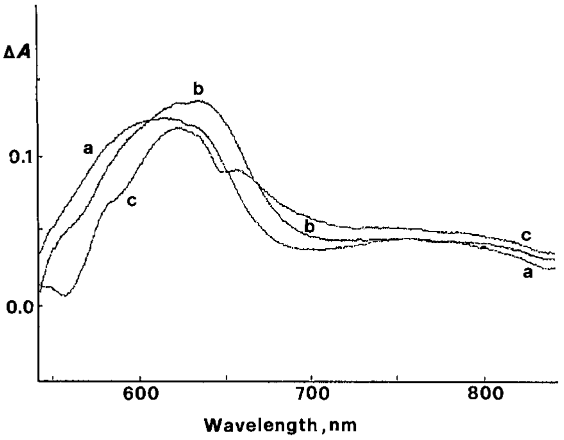

Figure 8. Differential transient absorption spectra at the end of a 35 ps pulse of butyronitrile solutions of **PAu** (a), **Ru–PAu** (b), and **PH_2-Ru-PAu** (c). Absorbance of solutions at the exciting wavelength are 0.21, 0.32 and 0.41, respectively.

The absorbance signal detected immediately after picosecond irradiation at 532 nm of an **Ru–PAu** dyad solution shows the typical bands of PAu triplet, decaying with a lifetime of 1,4 ns coincident with that of the model. No bands assignable to the radical anion of PAu^{III} formed by electron transfer from **Ru**, which absorbs around 735 nm,[28] could be detected under our experimental conditions (Figure 8b). It should be noted that differences at wavelengths shorter than 670 nm are assigned to the differences in ground state absorbances. The yield of PAu triplet formation was very similar for the dyad and the model indicating that the photons absorbed by the Ru moiety at 532 nm (30% if one takes an average of **Ru** and **Ru′** extinction coefficients) in the dyad populate the PAu triplet with unitary efficiency.

The absorbance signal detected immediately after picosecond irradiation of the **$Ru-PH_2$** dyad shows the bands of the free-base porphyrin singlet, which decays with a lifetime of 380 ps (Figure 9), in good agreement with the 400 ps luminescence lifetime. In parallel to the decay of the singlet there is an increase of the near-IR band typical of the triplet,[29] which is already present at the end of the pulse. The PH_2 triplet present immediately after the pulse is assigned to a rapid (faster than our instrumental resolution, $k > 5 \times 10^{10}$ s^{-1}) energy transfer from the ^{3}MLCT of the Ru complex. The Ru moiety in fact absorbs more than 50% of the incident light at 532 nm. The subsequent time evolution of the formed triplet can be followed by nanosecond-flash photolysis in air-free solutions in which a decay time of 40 µs is measured.

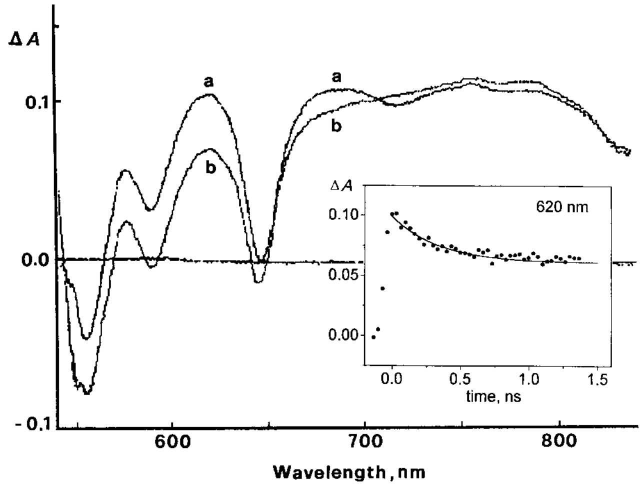

Figure 9. Differential transient absorption spectra, in the 540–840 nm region, of butyronitrile solutions of **$Ru-PH_2$** at the end of a 35 ps laser pulse (a), and 1.4 ns after the end of the pulse (b). The inset shows the decay of the absorbance at 620 nm and the exponential fit ($\tau = 380$ ps).

The increase in the intersystem-crossing rate to the ground state with respect to the model can be assigned to the effect of the Ru heavy atom. The calculated yield of the triplet in the dyad is close to unity, higher than the one in the model (Table 4 and Figure 10). This indicates that the energy absorbed by the Ru moiety at 532 nm (more than 50% if we take an average of **Ru** and **Ru′** absorption coefficients) is transferred to the PH_2 triplet with a close to unity yield, in agreement with the findings of the picosecond experiment.

Table 4. Transient absorbance in butyronitrile.

	STATE	τ [ns]	Φ_T
Ru	^{3}MLCT	0.7	
Ru′	^{3}MLCT	0.04	
PH_2	$^3PH_2$	2×10^5	0.61[a]
PAu	^{3}PAu	1.4	1.0[a]
$Ru-PH_2$	$^1PH_2$	0.38	
	$^3PH_2$	4×10^4	0.90[b]
Ru–PAu	^{3}PAu	1.4	1.0[b]
PH_2-Ru-PAu	^{3}PAu	1.4	0.95[b]
	$^3PH_2$	2×10^4	0.12[b]

[a] From ref. [19a]. [b] From $^3PH_2$ or ^{3}PAu absorbance at 680–700 nm, see experimental section.

The picosecond absorption spectrum on the triad **PH_2-Ru-PAu** excited at 532 nm shows, as the prominent feature immediately after the flash, the absorption spectrum of the PAu triplet (Figure 8c). The 440 nm band of the PH_2-localized excited singlet is overshadowed by the PAu triplet band at the same wavelength. No indication of the existence of other intermediates can be derived from our transient absorbance results. After the decay of the PAu triplet, which occurs with $\tau = 1.4$ ns, a residual absorption typical of the PH_2 triplet can

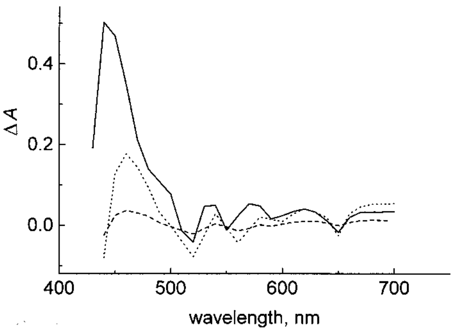

Figure 10. Differential transient absorption spectra after a 20 ns laser pulse of butyronitrile solutions of **PH_2** (—), **Ru – PH_2** (····) and **PH_2-Ru-PAu** (- - -). The absorbance of the solutions at the exciting wavelength was 0.15, 0.22, 0.4, respectively.

be detected by nanosecond-flash photolysis (Figure 10). In air-free solutions the lifetime of the PH_2-based triplet is 20 μs. An estimate of the porphyrin triplet yields (ϕ_T) gives a value of 0.95 for PAu and of 0.12 for PH_2. This is a clear indication that all the photons absorbed by the components of the triad convert to these triplet states. The successive decay to the ground state is unperturbed for the PAu-based triplet, while the rate of PH_2-based triplet decay is faster with respect to the model, probably because of some heavy-atom effect of the nearby ruthenium ion. The data derived from transient absorbance experiments are given in Table 4.

Photoinduced processes: Our interpretation of the above results is summarized in the energy diagrams of Figure 11, where the deactivation processes of the excited states at room temperature are reported. The energy levels of the charge-separated states (only the lowest one is reported for each dyad) are derived from the electrochemical potentials of Table 1 and the excited-state energies from the emission maxima at 77 K of Table 2. The **$^3PH_2$** energy level has been measured previously.[21]

Ru – PH_2* *dyad: In this dyad (Figure 11a) the lowest charge-separated state lies above the higher excited state of the system, and corresponds to the reduced metal complex unit and the oxidized porphyrin, **$Ru^- – PH_2^+$**. The electron-transfer processes to produce the charge-separated (CS) state are endergonic by approximately 0.2 eV, both approaching it from **Ru – $^1PH_2$**, the singlet localized on the porphyrin, or from **^3Ru – PH_2**, the excited state localized on the ^{3}MLCT of the Ru complex. The energy level of the latter, which could not be directly measured because of the absence of any emission from this moiety in the dyad, was assumed to be placed between the luminescent level of the **Ru** and **Ru′** models, that is, at about 2 eV.

Time-resolved luminescence and absorption experiments indicate that the **Ru – $^1PH_2$** state has a lifetime of 390 ps, and is therefore quenched with respect to the model ($\tau = 8.3$ ns) with a rate $k_1 = 2.4 \times 10^9$ s^{-1}.[30] Similarly we found that the luminescence of **^3Ru – PH_2** was also completely quenched and we derived a rate of $k_2 > 5 \times 10^{10}$ s^{-1} for this process. The excitation spectrum, measured with an emission wavelength equal to that of the the singlet porphyrin emission, is identical to the **PH_2** absorbance, therefore energy-transfer processes from the **^3Ru – PH_2** to **Ru – $^1PH_2$** can be excluded. We could not detect any transient feature ascribable to the CS state and, therefore, we assumed that none of the two quenching processes was due to electron transfer, but rather to energy-transfer steps. Energy transfer from **Ru – $^1PH_2$** to **^3Ru – PH_2**, that is, between states of different multiplicity, can occur because of the perturbed nature of the ^{3}MLCT state of the ruthenium complex, which is only formally a triplet. The mechanism can only be of Dexter type,[23] since dipole – dipole

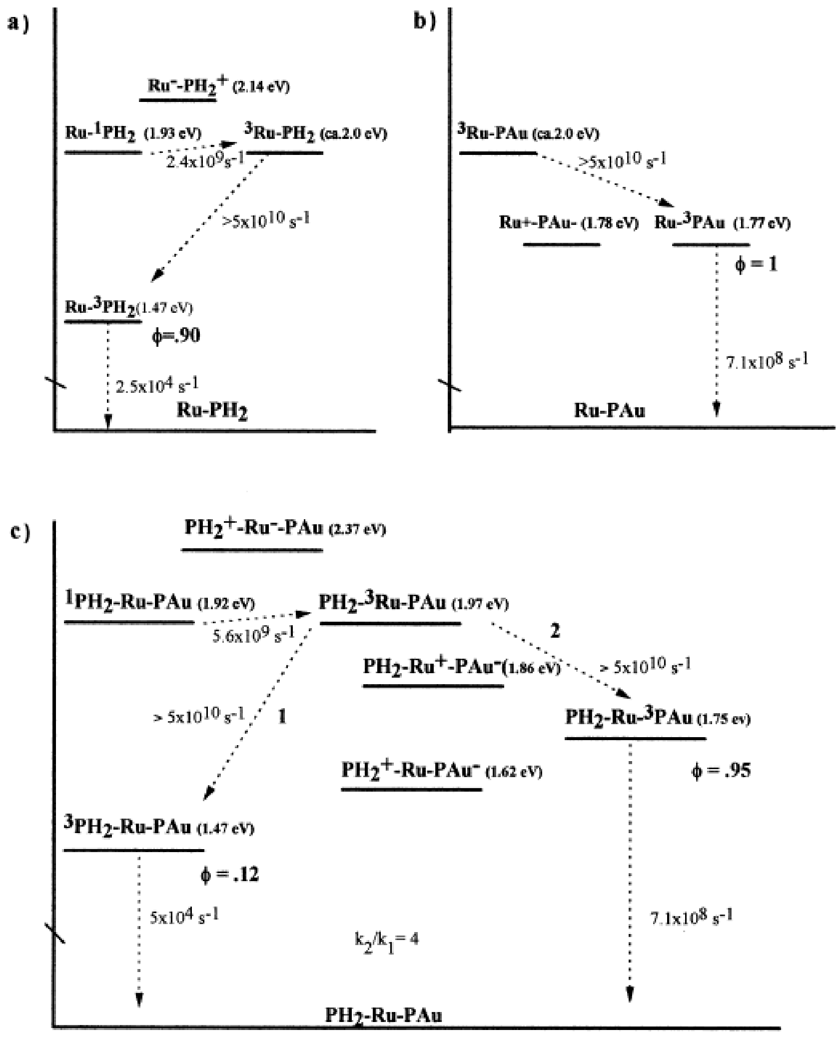

Figure 11. Schematic energy level diagrams for a) **Ru – PH_2**, b) **Ru – PAu** and c) **PH_2-Ru-PAu**. The partition of photons at 532 nm calculated on the basis of the absorption coefficients of the models is in **PH_2-Ru-PAu**: PH_2 20 %, Ru 30 %, PAu 50 %; in **Ru – PH_2**: Ru 55 %, PH_2 45 %; in **Ru-PAu**: Ru 30 %, PAu 70 %. In the dyads, an average of absorption coefficients of **Ru** and **Ru′** has been used.

interaction (Forster mechanism)[31] would require a sizable intensity for the electronic transition connecting the ground state to the sensitized state of the acceptor (i.e., from **Ru–PH$_2$** to **^{3}Ru–PH$_2$**), which is not the case.

Energy transfer by the Dexter mechanism can be envisaged as a double-electron exchange and can be treated by a formalism[32] similar to electron transfer.[33] In this framework, the relatively slow rate of energy transfer from **Ru–^{1}PH$_2$** to **^{3}Ru–PH$_2$** can be accounted for by the unfavourable driving force (ΔG slightly positive). The **^{3}Ru–PH$_2$** state is, in addition, immediately populated by intersystem-crossing from the **^{1}Ru–PH$_2$**, that is, the ^{1}MLCT localized on the Ru complex that is formed by direct absorption of 532 nm photons. From the **^{3}Ru–PH$_2$** state an extremely fast energy transfer to the porphyrin-localized **Ru–^{3}PH$_2$** triplet occurs. The yield of formation of the latter triplet is close to unity, indicating an efficient and complete, within experimental error, funnelling of the electronic energy to this state.[34] Energy transfer between triplets occurs by the Dexter mechanism, and it is not surprising that the **^{3}Ru–PH$_2$** → **Ru–^{3}PH$_2$** step, characterized by favourable thermodynamics ($\Delta G = -0.5$ eV; a small distance and a sizeable electronic coupling between donor and acceptor), occurs at rates faster than those previously reported for similar systems of the order of 3×10^9 s^{-1}.[19] The deactivation to the ground state of the **Ru–^{3}PH$_2$** occurs slightly faster than the model, probably because of the ruthenium heavy-atom effect on the intersystem-crossing rate.

***Ru–PAu** dyad*: In this dyad (Figure 11b) the lowest-energy CS state, corresponding to the reduced porphyrin and oxidized metal centre **Ru$^+$–PAu$^-$**, lies below the ^{3}MLCT level centred on the metal complex **^{3}Ru–PAu** and slightly above the **Ru–^{3}PAu**, the porphyrin-localized triplet. The quenching of **^{3}Ru–PAu** ($k > 5 \times 10^{10}$ s^{-1}) could, in principle, occur by electron transfer. We could not detect any intermediate attributable to this process, but we found a unitary yield of formation of **Ru–^{3}PAu**, indicating an efficient energy transfer between the ruthenium-complex- and the porphyrin-based triplets. The decay of **Ru–^{3}PAu** to the ground state occurs unperturbed with respect to the model PAu. The extremely fast triplet energy transfer occurring in this dyad can be explained, as in the previous case, by the occurrence of a Dexter-type energy transfer between a donor and acceptor closely coupled.

***PH$_2$-Ru-PAu** triad*: An additional state has to be considered in the triad (Figure 11c), with respect to those of the component dyads. This is the **PH$_2$$^+$-Ru-PAu$^-$** state, corresponding to the oxidation of free-base porphyrin and reduction of the gold(III) porphyrin. According to the electrochemical results this state is lower in energy than all the others involved, except for the triplet state localized on the free-base **^{3}PH$_2$-Ru-PAu**. From the experimental results, the quenching of **^{1}PH$_2$-Ru-PAu** occurs slightly faster ($k = 5.6 \times 10^9$ s^{-1}) than that detected for **^{1}PH$_2$–Ru**, probably because of a slightly less unfavourable driving force, and we ascribe it to energy transfer to **PH$_2$-^{3}Ru-PAu**, similar to that which happens in the dyad. The triplet so-formed undergoes a rapid deactivation ($k > 5 \times 10^{10}$ s^{-1}). We know from the behaviour of the dyads that both **^{3}PH$_2$-Ru-PAu** and **PH$_2$-Ru-^{3}PAu** can rapidly quench the triplet localized on the metal complex **PH$_2$-^{3}Ru-PAu.** The relative importance of the two paths described above can be derived from the ratio of the yields of the resulting products, 0.12 and 0.95 for **^{3}PH$_2$-Ru-PAu** and **PH$_2$-Ru-^{3}PAu**, respectively. For the latter a yield of 0.5 can be assigned to absorption at 532 nm by the PAu moiety and only the remaining 0.45 must be accounted for by energy transfer. As a consequence the ratio of the rates of energy transfer to the PAu- and PH$_2$-localized triplets is calculated to be four. The so-formed porphyrin triplet **PH$_2$-Ru-^{3}PAu** decays as for the model compound, while the other porphyrin triplet **^{3}PH$_2$-Ru-PAu** decays with a lifetime of 20 μs, reduced with respect to the same excited state in the model **^{3}PH$_2$** and in the dyad **Ru–^{3}PH$_2$**. This can be traced to a rather important heavy-atom effect, both from gold and ruthenium, on the intersystem-crossing rate of **^{3}PH$_2$-Ru-PAu** to the ground state. Neither electron transfer from the free base to the triplet state of the opposite PAu, nor triplet energy transfer from **PH$_2$-Ru-^{3}PAu** to **^{3}PH$_2$-Ru-PAu** could be detected, in spite of their exoergonicity. A similar behaviour was also noticed for less coupled systems,[19c] and was assigned to the inability of the interposed Ru-complex to promote efficient electronic coupling during the short lifetime of **^{3}PAu**. The unitary yield of triplets formed indicate that the energy-transfer processes discussed here can account for the total light absorbed and can satisfactorily describe the photoinduced processes occurring within this system.

Conclusions

It has been found that, in spite of the coupling of the components in the present multicomponent arrays, the systems can be described in terms of intramolecular processes between states localized on the individual components, which retain their properties with very small perturbations. The use of two different models for the metal complex core has allowed us to assess the pertinence of the model. Within this framework, the photophysical properties of a new ruthenium–terpyridine complex, bis(4′-methyl-2,2′:6′,2″-terpyridine)ruthenium(II), have been determined. The predominant role of energy-transfer processes in the deactivation of excited states of multicomponent arrays assembled on ruthenium metal complexes has been shown and is in agreement with our previous findings.[21–22] The occurrence of energy-transfer processes, which are formally forbidden on the basis of the spin multiplicity (i.e., from the free porphyrin based excited singlet to the ^{3}MLCT excited state localized on the ruthenium complex), is made possible by the heavy-atom-perturbing effect brought about by the ruthenium. We have shown that, when thermodynamically allowed, the energy transfer occurs and effectively competes with the even more exothermic electron-transfer processes. The energy transfer is thought to occur by a Dexter mechanism, which can be envisaged as a double-electron exchange. The reason for the prevalence of energy with respect to electron transfer can be found in the lower reorganisational energy required by an energy-transfer process in which no net charge transfer occurs, compared with electron transfer in which an electron is transferred from one site to another of the molecule, thereby requiring an higher solvent reorganization energy.

The investigated arrays have proved to be very efficient in performing energy-transfer processes. The occurrence of triplet energy migration between the extreme porphyrin components in the triad is probably precluded at room temperature by the short lifetime of the **^{3}PAu** donor. We intend to assess the occurrence of the Ru-complex-mediated energy transfer by an electron exchange mechanism in a glass, where the lifetime of the donor is greatly increased. In order to develop arrays of this type that are able to produce electron-transfer processes, one must consider the use of metal complexes with higher excited states and similar redox properties. We are currently working in this direction.

Experimental section

Synthesis: Reactions requiring an inert atmosphere or anhydrous conditions were carried out under a dynamic atmosphere of dry, oxygen-free argon. Dichloromethane was distilled under argon from P_2O_5 prior to use and pyrrole was purified by distillation at atmospheric pressure. All porphyrinic derivatives and ruthenium complexes were protected from light during chromatographic purification and during reactions. Thin layer chromatography (TLC) was carried out with aluminium oxide plates (aluminium-backed Merck Art 5550) or silica plates (glass-backed). Preparative column chromatography was carried out with neutral alumina (Merck Aluminium Oxide 90, activity II–III, 70–230 mesh) or with silica (Merck Silica Gel 60, 230–400 mesh). ^{1}H NMR spectra were recorded with a Bruker WP200SY, a Bruker AC250 or a Bruker AC300, referenced internally to residual protio-solvent resonances and reported relative to tetramethylsilane ($\delta = 0$). Coupling constants are quoted in Hertz. Mass spectra (FAB) were recorded on a VG ZAB-HF spectrometer and ESMS on a VG Platform.

4′-Formyl-2,2′:6′,2″-terpyridine: Methyl terpyridine (1g, 4 mmol) and selenium dioxide (2g, 18 mmol) were stirred vigorously in dioxane (80 cm^3) under reflux for 7 days. The progress of the reaction was readily monitored by TLC on alumina with an eluant of ethyl acetate/hexane (30:70). The R_f values of the starting material and product were 0.61 and 0.27, respectively. After the reaction had gone to completion, (according to TLC), the mixture was filtered and the dioxane removed under reduced pressure. The residue was dissolved in CH_2Cl_2, re-filtered and the solvent removed. Recrystallisation of the residue from hexane containing 5% dichloromethane yielded a colourless crystalline solid in 50% yield. The melting point and ^{1}H NMR spectrum match those reported previously for this compound prepared by a different procedure.[35, 19b]

5-[4′-(2,2′:6′,2″-terpyridyl)]tris[10,15,20-3,5-di-*tert*-butyl)phenyl]porphyrin: This compound was prepared according to the general procedures developed by Lindsey et al.[27] Formyl terpyridine (104.5 mg, 0.4 mmol) and 3,5-di-*tert*-butyl benzaldehyde (1.75g, 8 mmol) were dissolved in dichloromethane (600 cm^3) directly distilled from P_2O_5. Pyrrole (564 mg, 8.4 mmol, freshly distilled) was added, followed by trifluoroacetic acid (0.2 cm^3) and the mixture stirred under nitrogen for 2 h at room temperature in the dark. During this time, the solution turned a deep orange. DDQ was added (1.36g, 6 mmol) and the mixture stirred for a further 2 h at room temperature, during which time the solution became very dark. An excess of triethylamine was added and the solvent removed under reduced pressure. Purification was carried out by column chromatography on alumina (gradient elution from hexane to 20% diethyl ether/hexane). A second column was necessary in order to isolate the pure porphyrin in 11% yield. ($R_f = 0.45$ on alumina, ether/hexane = 30:70). ^{1}H NMR (200 MHz, $CDCl_3$, 25 °C): $\delta = 9.40$ (s, 2H), 8.97 (m, 2H), 8.95 (s and overlapping mutiplets, 8H), 8.67 (dd, J(H,H) = 4.3, 0.8 Hz, 2H), 8.12 (m, 6H), 8.00 (ddd, J(H,H) = 8.0, 8.0, 1.8 Hz, 2H), 7.81 (two t overlapping, J(H,H) = 1.8 Hz, 3H), 7.38 (ddd, J(H,H) = 7.5, 4.8, 1.1 Hz, 2H), 1.51 (s, 54H), −2.55 (s, 2H). (Note that a more highly resolved spectrum of this porphyrin recorded at 400 MHz allowing a full assignment has been reported previously[19b]); UV-Vis (CH_2Cl_2): λ_{max} (ε) = 648 (5300), 592 (4800), 554 (10000), 518 (17800), 421 nm (500000); MS (FAB+): m/z (%): 1106 (100) [M^++H].

[5-{4′-(2,2′:6′,2″-terpyridyl)}tris{10,15,20-(3,5-di-*tert*-butyl)phenyl}porphyrinato]aurate: The terpyridine-appended porphyrin (37 mg, 33 µmol) together with $KAuCl_4$ (32 mg, 83 µmol) and sodium acetate (22 mg, 264 µmol) were dissolved in acetic acid (5 cm^3). The resulting green solution was purged with nitrogen and then heated at reflux temperature under inert atmosphere for 40 h, the flask being wrapped in aluminium foil to shield from the light. The progress of the metallation reaction was monitored by visible absorption spectroscopy: the long wavelength Q bands in the free-base porphyrin (648 and 592 nm) were not present in the metalloporphyrin. After reaction, acetic acid was removed under reduced pressure and the residue taken up into dichloromethane. The solution was washed with Na_2CO_3 (10% aqueous solution) followed by a saturated aqueous solution of KPF_6 and finally water. After drying over anhydrous sodium sulfate, the solvent was removed and the crude product purified by column chromatography on alumina (gradient elution from dichloromethane to 10% methanol/dichloromethane). Yield 71%; ^{1}H NMR (200 MHz, $CDCl_3$, 25 °C): $\delta = 9.38$ (overlapping m, 10H), 9.00 (d, J(H,H) = 8.0 Hz, 2H), 8.65 (dd, J(H,H) = 3.9, 1.0 Hz, 2H), 8.09 (overlapping m, 8H), 7.93 (two overlapping t, J(H,H) = 2.0 Hz, 3H), 7.44 (ddd, J(H,H) = 7.4, 4.9, 1.2 Hz, 2H), 1.54 (s, 54H); UV-Vis (CH_2Cl_2): λ_{max} (ε) = 555(3100), 520 (18000), 415 nm (350000); MS (FAB+): m/z (%): 1300.9 (100) [M^+].

Triad PH$_2$-Ru-PAu: $RuCl_3 \cdot 3H_2O$ (5 mg, 19 µmol) was added to a suspension of the gold porphyrin (28 mg, 19 µmol) in absolute ethanol and the mixture heated at reflux for 4 h and was shielded from the light. The solvent was then removed under reduced pressure with mild heating only and the red residue obtained was re-dissolved in an acetone/ethanol mixture (15 cm^3:3 cm^3) in the presence of $AgBF_4$ (12 mg, 57 mmol). The mixture was heated gently to 50 °C for 3 h under argon, during which time a fine precipitate of AgCl appeared. This was removed by filtration over Celite and the Celite was washed with more acetone. Absolute ethanol (5 cm^3) was added to the combined filtrate and washings and the acetone subsequently removed selectively by rotary evaporation without heating. Free-base porphyrin (21.4 mg, 19 µmol) was added and the mixture heated at reflux under nitrogen for 4 h in the dark. The solvent was removed under reduced pressure and the residue re-dissolved in dichloromethane and washed with saturated KPF_6 (aq) to obtain the PF_6^- salt of the triad. The dichloromethane solution was dried over anhydrous sodium sulfate and the solvent removed. The crude product (30 mg) was purified by column chromatography on silica (60g) with a gradient elution from CH_3CN to $CH_3CN/H_2O/KNO_3$ (saturated aqueous solution, 95:5:0.02; $R_f = 0.35$ under these conditions). Following further anion exchange with KPF_6, the required triad was isolated in 20% yield. ^{1}H NMR (300 MHz, CD_2Cl_2, 25 °C): $\delta = 9.98$ (d, J(H,H) = 5.3 Hz, 2H), 9.65 (d, J(H,H) = 3.7 Hz, 4H), 9.55 (s, 2H), 9.42 (two t, J(H,H) = 5.5 Hz, 4H), 9.26 (d, J(H,H) = 4.8 Hz, 2H), 9.18 (d, J(H,H) = 4.8 Hz, 2H), 8.98 (s, 4H), 8.68 (d, J(H,H) = 8.1 Hz, 2H), 8.54 (d, J(H,H) = 8.1 Hz, 2H), 8.20 (dd, J(H,H) = 8.6, 1.3 Hz, 8H), 8.15 (d, J(H,H) = 4.8 Hz, 6H), 8.04 (m, 8H), 7.90 (d, J(H,H) = 1.8 Hz, 4H), 7.61 (dd, J(H,H) = 6.6 Hz, 2H), 7.51 (dd, J(H,H) = 6.6 Hz, 2H), 1.63 (s, 36H), 1.61 (s, 72H), −2.74 (s, 2H); UV-Vis (BuCN): data reported in Table 2; MS (FAB+): m/z (%): 2799 (67) [M^++(PF$_6$)$_2$], 2654 (36) [M^++(PF$_6$)], 2507 (75) [M^+].

Dyad Ru-PH$_2$: Ruthenium methyl terpyridine trichloride was prepared by a procedure analogous to that used for the tolylterpyridine compound.[36] Thus, methylterpyridine (50 mg, 0.2 mmol) and $RuCl_3 \cdot 3H_2O$ (52 mg, 0.2 mmol) were heated together in absolute ethanol (15 cm^3) under reflux for 4 h and the red-brown precipitate which formed was separated by filtration and washed successively with ethanol, toluene and ether. A suspension of the trichloride (9 mg, 19.8 µmol) in a mixture of acetone and absolute ethanol (8 cm^3:2 cm^3) was heated at reflux in the presence of $AgBF_4$ (11.7 mg, 59.4 µmol) for 3 h under nitrogen. The fine precipitate of AgCl was removed by filtration over Celite and ethanol (absolute, 4 cm^3) was added to the dark purple filtrate. The acetone was selctively removed by rotary evaporation without heating. Free-base porphyrin was added (22 mg, 19.8 µmol) and the ethanol solution then heated under nitrogen at reflux temperature for 4 h in the dark. Subsequently, the solvent was removed and the residue redissolved in dichloromethane and subjected to anion exchange with KPF_6 (aq) as described for the triad. The crude product was purified by chromatography on silica under conditions analogous to those used for the triad. Yield 7 mg (24 %); ^1H NMR (200 MHz, CD_2Cl_2, 25 °C): $\delta = 9.47$ (s, 2 H), 9.23 (d, J(H,H) = 4.7 Hz, 2 H), 9.15 (d, J(H,H) = 4.9 Hz, 2 H), 8.98 (s, 4 H), 8.62 (s, 2 H), 8.51 (d, J(H,H) = 7.9 Hz, 2 H), 8.45 (d, J(H,H) = 7.6 Hz, 2 H), 8.17 (d, J(H,H) = 1.9 Hz, 4 H), 8.13 (d, J(H,H) = 1.7 Hz, 2 H), 8.02 (ddd, J(H,H) = 7.9, 7.9, 1.5 Hz, 2 H), 7.90 (overlapping mutiplets, 6 H), 7.73 (d, J(H,H) = 4.7 Hz, 2 H), 7.55 (d, J(H,H) = 4.7 Hz, 2 H), 7.42 (ddd, J(H,H) = 6.5, 1.3, 1.3 Hz, 2 H); 7.33 (ddd, J(H,H) = 6.4, 1.3, 1.3 Hz, 2 H): UV-Vis (BuCN): data reported in Table 2; MS (ES +): m/z (%): 1599.3 (3) $[M^+ + (PF_6)]$, 727,1 (100) $[M^{2+}]$.

Dyad Ru – PAu: The gold dyad **Ru – PAu** was prepared in an analogous manner from ruthenium methylterpyridine trichloride and the gold porphyrin. UV-Vis bands in butyronitrile are reported for both dyads in Table 2.

Bis(methylterpyridine)ruthenium(II) hexafluorophosphate (**Ru′**): Ruthenium methylterpyridine trichloride (30 mg, 66 μmol) was heated in acetone (5 cm^3) in the presence of silver triflate (51 mg, 198 μmol) for 3 h and the silver chloride precipitate removed by filtration through Celite. Absolute ethanol was added (4 cm^3) and the acetone removed selectively by rotary evaporation. Methylterpyridine (16 mg, 66 μmol) was then added and the ethanolic solution heated under reflux for 4 h. The rutheniumbis(methylterpyridine) was isolated as its triflate salt by recrystallisation from ethanol. Anion exchange was subsequently performed with KPF_6 as described for the dyad **Ru – PH$_2$**. Yield = 15 mg (38 %); ^1H NMR (250 Hz, CD_3CN, 25 °C): $\delta = 8.73$ (s, 4 H), 8.54 (m, 4 H), 8.01 (ddd, J(H,H) = 8.3, 8.3, 1.4 Hz, 4 H), 7.42 (m, 4 H), 7.25 (ddd, J(H,H) = 7.6, 5.7, 1.5 Hz, 4 H), 3.01 (s, 6 H); ^{13}C NMR (62.9 MHz, CD_3CN, 25 °C): $\delta = 22.0$ (CH_3) 125.0, 125.4, 128.2, 138.9 (aryl CH, outer pyridyls), 149.2 (C – Me), 153.3 (aryl CH, centre pyridyl), 155.8, 159.1 (quaternary C); UV-Vis (BuCN): data are reported in Table 2; MS (ES +): m/z (%): 298.1 (100) $[M^{2+}]$.

[{5,10,15,20-(3,5-di-*tert*-butyl)phenyl}porphyrinato]aurate (**PAu**): This compound was prepared by metallation of the symmetrical porphyrin PH_2 under the experimental conditions described previously.[37]

Electrochemical measurements: Experiments were performed on a PAR model 273A potentiostat with a three-electrode system in butyronitrile containing 0.1 M nBu_4NBF_4 as supporting electrolyte. The working electrode was a platinum disk. The potentials values were determined by cyclic voltammetry at a scan rate of 100 mVs^{-1} and were reported versus a saturated potassium chloride calomel electrode (SCE).

Spectroscopic and photophysical measurements: The solvent used was butyronitrile (Fluka). Absorption spectra were recorded at room temperature with a Perkin – Elmer Lambda 5 spectrophotometer. Uncorrected emission spectra were obtained with a Spex Fluorolog II spectrofluorimeter, equipped with a Hamamatsu R-928 photomultiplier tube. The delayed luminescence spectra of gold(III) porphyrin triplets were recorded by the same spectrofluorimeter equipped with a 1934D phosphorimeter accessory (Spex). Spectra at 77 K were measured from quartz capillary tubes immersed in a home-made quartz dewar filled with liquid nitrogen. An IBH single-photon counting apparatus ($\lambda_{exc} = 337$ nm, 1 ns time resolution) and a system based on a Nd:YAG laser and a Hamamatsu C1587 streak camera ($\lambda_{exc} = 532$ nm, 20 ps time resolution) were used to detect fluorescence lifetimes. Streak images were used to detect the **Ru′** spectral profile at room temperature. Experimental details are reported elsewhere.[38a] Nanosecond-flash-photolysis studies were made with the second harmonic of a Nd:YAG laser, the energy was 1 – 2 mJ per pulse. Samples were degassed by freeze-and-pump cycles. Details on the experimental setup have been reported previously.[38b,c] Transient absorption spectra in the picosecond time domain were measured by a pump-and-probe system. The second harmonic of a Nd:YAG laser (Continuum PY62-10) with a 35 ps pulse was used to excite the samples with energy ranging from 2 to 5 mJ. Further details on the experimental set-up and the treatment of data are reported elsewhere.[22] Yields of formation of the porphyrin triplets (Φ_T) in the dyads and the triad were determined by comparing the transient absorbances at 680 – 700 nm, wavelength out of ground state absorbance, with the corresponding values of the model compounds **PH$_2$** and **PAu**, and making corrections for the fraction of light absorbed at 532 nm by the samples. It was assumed that the molar absorption coefficients of triplets are unaffected in passing from models to the arrays. The spectroscopic energies of the electronic levels of the various compounds were derived from the maxima of the luminescence bands at 77 K. Experimental uncertainties are estimated to be 8 % for lifetime determination, 10 % for quantum yields, 20 % for molar absorption coefficients and 3 nm for emission and absorption peaks. The working temperature is 298 K, unless otherwise stated.

Acknowledgments: We thank Gian Marco Rossetti for his help in some experiments. Italian C.N.R. and French C.N.R.S. supported this work. The Royal Society is thanked for a fellowship (to J.A.G.W.) under the European Science Exchange Programme.

Received: January 19, 1998 [F 967]

---

[1] For recent reviews : a) M. R Wasielewski, *Chem. Rev.* **1992**, *92*, 435; b) D. Gust, T. A. Moore, A. L. Moore, *Acc. Chem. Res.* **1993**, *26*, 198; c) H. Kurreck, M. Huber, *Angew. Chem.* **1995**, *107*, 929; *Angew. Chem. Int. Ed. Engl.* **1995**, *34*, 849; d) A. Harriman, J.-P. Sauvage, *Chem. Soc. Rev.* **1996**, 41; e) H. Imahori, Y. Sakata, *Adv. Mater.* **1997**, *9*, 537; f) D. Gust, T. A. Moore, A. L. Moore, *Res. Chem. Intermed.* **1997**, *23*, 621; g) A. P. de Silva, H. Q. N. Gunaratne, T. Gunnlaugsson, A. J. M. Huxley, C. P. McCoy, J. T. Rademacher, T. E. Rice, *Chem. Rev.* **1997**, *97*, 1515.

[2] a) R. W. Wagner, T. E. Johnson, J. S. Lindsey, *J. Am. Chem. Soc.* **1996**, *118*, 11166; b) F. Li, S. Gentemann, W. A. Kalsbeck, J. Seth, J. S. Lindsey, D. Holten, D. F. Bocian, *J. Mater. Chem.* **1997**, *7*, 1245.

[3] M. G. Ranasinghe, A. M. Oliver, D. F. Rothenfluh, A. Salek, M. N. Paddon-Row, *Tetrahedron Lett.* **1996**, *37*, 4797.

[4] a) A. Osuka, S. Nakajima, K. Marujama, N. Mataga, T. Asahi, I. Yamazaki, Y. Nishimura, T. Ohno, K. Nozaki, *J. Am. Chem. Soc.* **1993**, *115*, 4577; b) A. Osuka, S. Marumo, N. Mataga, S. Taniguchi, T. Okada, I. Yamazaki, Y. Nishimura, T. Ohno, K. Nozaki, *J. Am. Chem. Soc.* **1996**, *118*, 155; c) A. Osuka, S. Nakajima, T. Okada, S. Taniguchi, K. Nozaki, T. Ohno, I. Yamazaki, Y. Nishimura, N. Mataga, *Angew. Chem.* **1996**, *108*, 98; *Angew. Chem. Int. Ed. Engl.* **1996**, *35*, 92.

[5] a) P. A. Lidell, D. Kuciauskas, J. P. Sumida, B. Nash, D. Nguyen, A. L. Moore, T. A. Moore, D. Gust, *J. Am. Chem. Soc.* **1997**, *119*, 1400; b) D. Kuciauskas, P. A. Lidell, S.-C. Hung, S. Lin, G. R. Seely, A. L. Moore, T. A. Moore, D. Gust, *J. Phys. Chem.* **1997**, *101*, 429; c) Q. Tan, D. Kuciauskas, S. Lin, S. Stone, A. L. Moore, T. A. Moore, D. Gust, *J. Phys. Chem.* **1997**, *101*, 5214; d) A. A. Krasnowsky, Jr., M. E. Bashtanov, N. N. Drozdova, P. A. Lidell, A. L. Moore, T. A. Moore, D. Gust, *J. Photochem. Photobiol. A* **1997**, *102*, 157.

[6] G. P. Wiederrecht, M. P. Niemczyk, W. A. Svec, M. R. Wasielewski, *J. Am. Chem. Soc.* **1996**, *118*, 81.

[7] C. Turrò, C. K. Chang, G. E. Leroi, R. I. Cukier, D. G. Nocera, *J. Am. Chem. Soc.* **1992**, *114*, 4013.

[8] a) J. L. Sessler, B. Wang, A. Harriman, *J. Am. Chem. Soc.* **1993**, *115*, 10418; b) J. L. Sessler, B. Wang, A. Harriman *J. Am. Chem. Soc.* **1995**, *117*, 704; c) T. Arimura, C. T. Brown, S. L. Springs, J. L. Sessler, *Chem. Commun.* **1996**, 2293.

[9] a) C. A. Hunter, R. K. Hyde, *Angew. Chem.* **1996**, *108*, 2064; *Angew. Chem. Int. Ed. Engl.* **1996**, *35*, 1936; b) C. A: Hunter, R. J. Shannon, *Chem. Commun.* **1996**, 1361.

[10] T. Hayashi, T. Miyahara, S. Kumazaki, H. Ogoshi, K. Yoshihara, *Angew. Chem.* **1996**, *108*, 2096; *Angew. Chem. Int. Ed. Engl.* **1996**, *35*, 1964.

[11] H. Imamori, E. Yoshizava, K. Yamada, K. Hagiwara, T. Okada, Y. Sakata, *J. Chem. Soc. Chem. Commun.* **1995**, 1133.

[12] F. D'Souza, G. R. Deviprasad, Y.-Y. Hsieh, *Chem. Commun.* **1997**, 533.

[13] C. A. Drain, K. C. Russel, J.-M. Lehn, *Chem. Commun.* **1996**, 337.

[14] a) Y. Kuroda, A. Kawashima, Y. Hayashi, H. Ogoshi, *J. Am. Chem. Soc.* **1997**, *119*, 4929; b) T. Hayashi, T. Miyahara, N. Koide, Y. Kato, H. Masuda, H. Ogoshi, *J. Am. Chem. Soc.* **1997**, *119*, 7281.

[15] a) T. Haberle, J. Hirsh, F. Pöllinger, H. Heitele, M. E. Michel-Beyerle, C. Anders, A. Döhling, C. Krieger, A. Rückermann, H. A. Staab, *J. Phys. Chem.* **1996**, *100*, 18269; b) F. Pöllinger, C. Musewald, H. Heitele, M. E. Michel-Beyerle, C. Anders, M. Futscher, G. Voit, H. A. Staab, *Ber. Bunsen-Ges. Phys. Chem.* **1996**, *100*, 2076.

[16] H. Imamori, K. Hagiwara, M. Aoki, T. Akiyama, S. Taniguchi, T. Okada, M. Shirakava, Y. Akiyama, *J. Am. Chem. Soc.* **1996,** *118*, 11771.

[17] T. D. M. Bell, T. A. Smith, K. P. Ghiggino, M. G. Ranashinghe, M. J. Shepard, M. N. Paddon-Row, *Chem. Phys. Lett.* **1997**, *268,* 223.

[18] J.-S. Hsiao, B. P. Krueger, R. W. Wagner, T. E. Johnson, J. K. Delaney, D. C. Mauzerall, G. R. Fleming, J. S. Lindsey, D. F. Bocian, R. J. Donohoe, *J. Am. Chem. Soc.* **1996,** *118*, 11181.

[19] a) A. M. Brun, A. Harriman, V. Heitz, J.-P. Sauvage, *J. Am. Chem. Soc.* **1991,** *113*, 8657; b) J.-P. Collin, A. Harriman, V. Heitz, F. Obodel, J.-P. Sauvage, *J. Am. Chem. Soc.* **1994,** *116*, 5679; c) A. Harriman, F. Obodel, J.-P. Sauvage *J. Am. Chem. Soc.* **1995,** *117*, 9461.

[20] F. Obodel, J.-P. Sauvage, *New J. Chem*. **1994**, *18*, 1139.

[21] J.-P. Collin, J.-O. Dalbavie, V. Heitz, J.-P. Sauvage, L. Flamigni, N. Armaroli, V. Balzani, F. Barigelletti, I. Montanari, *Bull. Soc. Chim. Fr.* **1996**, *133*, 749.

[22] L. Flamigni, N. Armaroli, F. Barigelletti, V. Balzani, J.-P. Collin, J.-O. Dalbavie, V. Heitz, J.-P. Sauvage, *J. Phys. Chem. B* **1997**, *101*, 5936.

[23] D. L. Dexter, *J. Chem. Phys.* **1953,** *21*, 836.

[24] J.-P. Sauvage, J.-P. Collin, J.-C. Chambron, S. Guillerez, C. Coudret, V. Balzani, F. Barigelletti, L. De Cola, L. Flamigni, *Chem. Rev.* **1994**, *94*, 993.

[25] M. Maestri, N. Armaroli, V. Balzani, E. C. Constable, A. M. W. Cargill Thompson, *Inorg. Chem.* **1995**, *34*, 2759.

[26] F. Barigelletti, L. Flamigni, J.-P. Collin, J.-P. Sauvage, *Chem. Commun*. **1997**, 333.

[27] J. S. Lindsey, H. C. Hsu, I. C. Schreiman, *Tetrahedron Lett*. **1986**, *27*, 4969.

[28] M. E. Jamin, R. T. Iwamoto, *Inorg. Chim. Acta* **1978**, *27*, 135.

[29] J. Rodriguez, C. Kirmaier, D. Holten, *J. Am. Chem. Soc.* **1989,** *111*, 6500.

[30] The quenching rate is calculated from the equation: $k = 1/\tau - 1/\tau_0$, where τ_0 is the lifetime of the state in the model, that is, in absence of quenching.

[31] Th. H. Forster, *Discuss. Faraday Soc*. **1959**, *27*, 7.

[32] a) V. Balzani, F. Bolletta, F. Scandola, *J. Am. Chem. Soc*. **1980**, *102*, 2152; b) N. Sutin, *Acc. Chem. Res.* **1982**, *15*, 275; c) F. Scandola, V. Balzani, *J. Chem. Educ.* **1983**, *60*, 814.

[33] R. A. Marcus, N. Sutin, *Biochim. Biophys. Acta* **1985**, *811*, 265.

[34] A simple increase in the intersystem-crossing rate of free-base porphyrin singlet to triplet, induced by the ruthenium heavy-atom effect, would be of relevance only to the photons absorbed by the porphyrin moiety (50%) and would not account for a unity yield, which requires an energy transfer from the ruthenium-localized ^{3}MLCT state.

[35] E. Vismara, F. Fontana, F. Minisci, *Gazz. Chim. Ital*. **1987**, *117*, 135.

[36] J.-P. Collin, S. Guillerez, J.-P. Sauvage, F. Barigelleti, L. De Cola, L. Flamigni, V. Balzani, *Inorg. Chem*. **1991**, *30*, 4230.

[37] V. Heitz, J.-P. Sauvage, *Tetrahedron Lett*. **1991**, *32*, 197.

[38] a) L. Flamigni, *J. Phys. Chem.* **1993**, *97*, 9566; b) L. Flamigni, *J. Phys. Chem.* **1992**, *96*, 3331; c) L. Flamigni, *J. Chem. Soc. Faraday Trans.* **1994**, *90*, 2331.